

# Technical Report

Department of Computer Science  
and Engineering  
University of Minnesota  
4-192 Keller Hall  
200 Union Street SE  
Minneapolis, MN 55455-0159 USA

TR 14-002

Pursuit and Evasion with Uncertain Bearing Measurements

Joshua Vander Hook and Volkan Isler

January 07, 2014



1 Pursuit and Evasion with Uncertain Bearing Measurements  
2 [Technical Report]

3 Josh Vander Hook and Volkan Isler\*

4 January 6, 2014

5 **Abstract**

6 We study pursuit-evasion games in which a pursuer tries to capture an evader by moving on to the  
7 evader's current location. We investigate how sensing capability of the pursuer affects the game outcome.  
8 In particular, we consider a pursuer which can sense only the bearing to an evader. Furthermore, there  
9 is noise in the measurements in such a way that an adversary may adjust each bearing measured by an  
10 angle up to  $\alpha$  away from the true value.

11 In this work, we study two classical pursuit evasion games under bearing uncertainty. In the first  
12 game, played on the open plane, the pursuer tries to maintain the distance to an evader with equal speed.  
13 If the pursuer has full knowledge of the evaders location the pursuer can maintain the separation between  
14 the players by moving toward the evader. However, when an adversarial sensing model is introduced, we  
15 show that for any pursuer strategy, the evader can increase the distance to the pursuer indefinitely. The  
16 rate at which the distance increases is linear in time.  $\alpha$ .

17 In the second game, both players are inside a bounded circular area. This version is known as the  
18 Lion-and-Man game, and has been well studied when no sensing limitations are imposed. In particular,  
19 the pursuer (Lion) is known to have an  $O(r \log r)$  strategy to capture the evader, where  $r$  is the radius of  
20 the circle. In contrast, when sensing uncertainty is introduced, we show that for any  $\alpha > 0$ , there exist  
21 environments in which the man can evade capture indefinitely.

---

\*The authors are with the Department of Computer Science and Engineering at the University of Minnesota. Emails: {jvander, isler}@cs.umn.edu



Figure 1: The robots designed for tracking fish during the winter (left) and summer (middle). The direction-sensitive antenna mounted on the robots (right). The bearing to the target can be estimated by rotating the antenna every  $\alpha$  degrees. The bearing corresponding to the maximum signal strength is taken as the true bearing. Thus, the uncertainty is at most  $\alpha$ .

## 1 Introduction

In a typical pursuit-evasion game, a pursuer tries to capture an evader who in turn tries to avoid capture. Earlier pursuit-evasion games were studied as recreational mathematics problems. For example, in the lion-and-man game presented in [1] a lion tries to capture a man in a circular arena. In recent years, pursuit-evasion games have received significant attention due to their applications in robotics and related fields [2].

In the last couple of years, our group has been working on building a system of autonomous boats for tracking radio-tagged invasive fish [3]. In our system, each boat can rotate its directional antenna to measure the bearing of a fish. See Figure 1. The goal is to track the movement of the fish using these measurements. Modeling such tracking problems as pursuit-evasion games is advantageous because we do not have good models for how the fish move. By modeling the targets as adversaries that are trying to escape and designing corresponding pursuit strategies, we can obtain tracking strategies which work regardless of the motion of the fish.

For such pursuit strategies to be practically applicable, they must work under realistic sensing models. Unfortunately, traditional formulations assume idealized measurements. For example, in the lion-and-man game mentioned above, the lion can obtain the exact location of the man at all times. In contrast, in most robotics settings the location of the target is not available. In our fish tracking application, the pursuer can measure only the bearing rather than the exact location. Moreover, the measurements are uncertain: if we rotate the antenna  $\alpha$  degrees between consecutive measurements and obtain the angle with the highest signal value, our estimate of the bearing can be off by  $\alpha$  degrees.

In this work, we study pursuit-evasion games in which the pursuer can obtain only uncertain bearing measurements. Bearing sensors, in particular cameras and microphone arrays, are commonly used in robotics and sensor network applications. Therefore, the setting we study arises in many applications. We provide two surprising results.

First, we look into the simple setting of chasing the evader in the open plane. When the players have the same maximum speed, the best pursuer can do is to maintain the initial distance between the players by moving toward the evader along the line connecting them. The evader can ensure that the separation is maintained by moving away from the pursuer in the same direction. The pursuer can execute this strategy even if he obtains only bearing measurements (rather than the exact location of the evader). In Section 2, we show that, if the bearing measurements are uncertain, the evader can increase the distance between the players! Specifically, we show that for any pursuer strategy, there exists an evasion strategy which guarantees that the distance between the players increases indefinitely.

Second, we study the lion-and-man game in a circular arena. Intuitively, it is easy to see that the pursuer can get closer and closer to the evader by moving toward it. This is because, the evader has to move away

56 from the pursuer to maintain separation. However, this is not possible indefinitely in a bounded arena.  
 57 Every time the man turns, the distance between the players decreases. Note that this greedy strategy can  
 58 be executed even when the pursuer can obtain only bearing measurements<sup>1</sup>. In Section 3, we show that the  
 59 outcome favors the evader if there is uncertainty in the measurements. We show that, for any uncertainty  
 60 value  $\alpha$ , there are circular environments in which the evader can escape by presenting an evasion strategy.

61 There are very few theoretical results regarding pursuit-evasion with sensing uncertainty. A notable  
 62 exception is the result by R ote who studied the problem of chasing the target in the open plane [5]. In his  
 63 model, the evader can hide its true location and present any location within distance  $d$  from his true location  
 64 as the measurement. It was shown that the evader can increase his distance from the pursuer at a rate of  
 65  $\Theta(\sqrt[3]{t})$ , where  $t$  is the time spent playing. In case of bearing measurements, we show that the evader can do  
 66 much better and ensure that the increase in the distance is linear in  $t$ .

67 In the next section, we start by studying the game on the open plane. For convenience, in the appendix  
 68 we present notation and explanations of variables used throughout the paper.

## 69 2 Open Plane Pursuit

70 In this section we describe the evader’s strategy to win the open-plane pursuit. We first cover the game  
 71 model. Let the position of the evader and pursuer at the beginning of turn  $t$  be  $e(t)$  and  $p(t)$  respectively.  
 72 Each turn proceeds as follows. First, the pursuer measures the angle  $b(t) = b^*(t) + \alpha(t)$ , where  $b^*(t)$  is the  
 73 true bearing to the evader and  $\alpha(t)$  is the offset applied by the evader, subject to  $|\alpha(t)| \leq \alpha$ . Next, the  
 74 pursuer chooses his next location  $p(t+1)$  subject to  $\|p(t+1) - p(t)\| \leq 1$ . The strategy by which the pursuer  
 75 chooses his next location is given by the policy  $\pi : (P, B) \rightarrow p(t+1)$ , where  $P = \{p(1), p(2), \dots, p(t)\}$  is the  
 76 previous pursuer positions, and  $B = \{b(1), b(2), \dots, b(t)\}$  is all the measurements received by the pursuer.  
 77 Next, the evader moves to  $e(t+1)$  where  $\|e(t+1) - e(t)\| \leq 1$ .

### 78 2.1 Evader Strategy

79 We will show that *for any* policy  $\pi$ , the evader can specify a trajectory and measurement sequence to  
 80 increase the distance between the pursuer and evader. Let  $\pi_p$  be the pursuer’s specified strategy. The  
 81 evader strategy proceeds in rounds, each consisting of  $N$  turns. The evader will first *simulate* a possible  
 82 measurement sequence,  $B$ , and observe the output of the policy  $\pi_p(P, B)$  (i.e., the pursuer’s trajectory).  
 83 Based on the pursuer’s trajectory, the evader will choose a trajectory to follow, but will use the same  
 84 measurement sequence,  $B$ , used in the simulation step. Since the pursuer’s response is a function of the  
 85 *measurements* and not the evader’s position, the evader can follow a different trajectory without altering the  
 86 pursuer response, as long as the measurements remain the same.

As shown in Figure 3 let the line  $\overline{p(0)e(0)}$  be the  $x$  axis of a coordinate frame which remains fixed for  
 the current round. Let  $d(0)$  be the separation between  $p(0)$  and  $e(0)$  at the beginning of the round. There  
 are two parameters to the simulation, a constant  $T_\alpha$  and  $\rho$ . Here,  $N = T_\alpha \cdot \frac{d(0)}{\rho}$  is the length of the round  
 (in turns) and is specified by the evader, and  $\rho$  is an acute angle (offset from  $\overline{p(0)e(0)}$ ) which is less than  $\alpha$ .  
 $T_\alpha$  is given as follows (and is derived in Theorem 1). The value of the constant  $T_\alpha$  was chosen to maximize  
 the final distance at the end of the round (as a function of  $\alpha$ )

$$T_\alpha = \left(1 - \sqrt{\frac{1}{2 - 2 \cos \alpha}}\right)^{-1} \quad (1)$$

Given  $T_\alpha$ , we solve for  $\rho$  (consulting Figure 2) using the triangle formed by the points  $e(0)$ ,  $p^*(N)$ , and  $e(N)$ .  
 This yields,

$$\rho = \pi - \sin^{-1} \left( (1 - T_\alpha^{-1}) \sin \alpha \right) \quad (2)$$

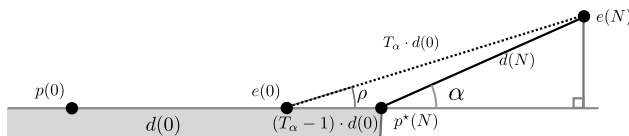


Figure 2: With a pursuer at starting location  $p(0)$  and evader at  $e(0)$ , with separation  $d(0)$ , the evader's strategy makes use of a *simulation step* to ensure after  $N = T_\alpha \cdot d(0)$  turns, the pursuer  $p(N)$  and evader  $e(N)$  are on opposite sides of the line  $\overline{p(0)e(0)}$ . Thus, the pursuer can be anywhere in the lower half circle of radius  $N$  (shaded portion), and the evader is at location  $e(N)$ . The closest position the pursuer can take is at  $p^*(N)$ , and the ending distance between the players is given by  $d(N)$ .

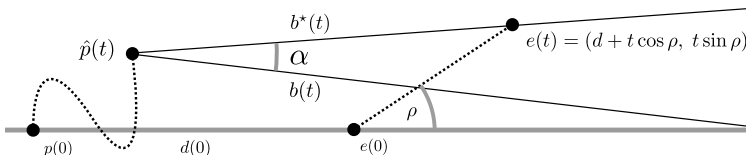


Figure 3: The evader's simulation, which is used to find the final pursuer's location after  $N$  steps, given measurement sequence  $B$ . The evader path is shown along with one possible pursuer path. The true bearing ( $b^*(t)$ ) and offset bearing ( $b(t)$ ) are solid lines.

87 The specific steps of the simulation are given in Algorithm 1, and illustrated in Figure 3. The evader will  
 88 calculate the pursuer's simulated location,  $\hat{p}$  as a function of the declared strategy,  $\pi_p$  for  $N = T_\alpha \cdot d(0)$  steps.  
 89 To construct an input measurement for each turn, the evader will first find  $b^*(t)$ , the orientation of the line  
 90  $\overline{\hat{p}(t)e(t)}$ , where  $e(t) = (d + t \cos \rho, t \sin \rho)$  for each turn  $t \in [1, N]$ . Then, the sequence  $B = \{b(1), \dots, b(N)\}$   
 91 is given by  $b^*(t) - \alpha$  for all  $N$  steps.

92 At the end of the simulation, the evader knows the pursuer's final location after  $N$  steps,  $\hat{p}(N)$  as a  
 93 response to the measurement sequence  $B$ . The goal of the evader's strategy is to move to a final position  
 94  $e(N)$  which is on the opposite side of  $\overline{p\hat{e}}$  as the final pursuer position,  $\hat{p}(N)$ . We separate the result into two  
 95 cases, and show in both cases the desired result is possible.

96 **Case 1.** The final simulated pursuer position,  $\hat{p}(N)$ , is on or below the line  $\overline{p\hat{e}}$

97 In this case the evader will move along the path specified by  $e(t) = (d + t \cos \rho, t \sin \rho)$ , and generate  
 98 bearing measurements  $B$ . Since the input does not change from the simulation,  $p(N)$  will be  $\hat{p}(N)$ , and the  
 99 final position of the evader will be  $(d + N \cos \rho, N \sin \rho)$ .

100 **Case 2.** The final simulated pursuer position,  $\hat{p}(N)$ , is above the line  $\overline{p\hat{e}}$

101 In this case, the evader will follow a different trajectory,  $E'$  which is the reflection of  $E$  about  $\overline{p\hat{e}}$ . Or,  $e(t)$   
 102 is the point  $(d + t \cos \rho, -t \sin \rho)$  for all  $t \in [1, N]$ . Assuming  $B$  does not change, the pursuer will again follow  
 103 the simulated output,  $\hat{p}$ , and arrive at  $p(N)$  at the end of the round, this case is similar to the previous case:  
 104 Both pursuer and evader are on the opposite side of  $\overline{p\hat{e}}$ . We now show the bearing measurements  $B$ , do not  
 105 need to change while the evader is moving along the path  $E'$ . To proceed, we need the following structural  
 106 lemma.

107 **Lemma 1.** As shown in Figure 4(a), let  $\ell_1$  and  $\ell_2$  be two parallel lines separated by perpendicular distance  
 108  $d$ . Place any two non-coincident points on  $\ell_2$ ,  $p_1$  and  $p_2$ , separated by distance  $s > 0$ . Now consider a third  
 109 point at distance  $d$  or greater from  $\ell_2$ ,  $x$ . The function  $\beta(x) = \overline{p_1 x p_2}$  is maximized at  $x^*$ , which is at distance  
 110  $d$  along the perpendicular bisector of  $p_1$  and  $p_2$ .

<sup>1</sup>This is not the most efficient pursuit strategy. Alonso et al. present a near optimal strategy for capture [4]. Their strategy however requires measuring the exact location of the man.

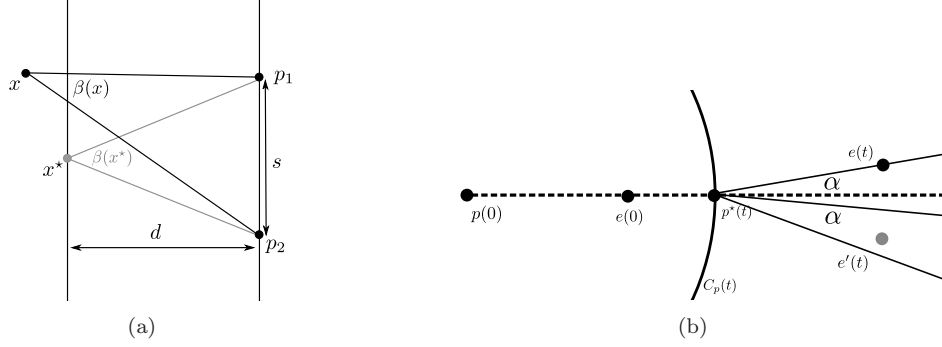


Figure 4: **a)** An illustration of Lemma 1: The angle  $\widehat{p_1 x p_2}$ , labelled  $\beta(x)$ , is maximized at the distance  $d$  along the perpendicular bisector of  $p_1$  and  $p_2$ . **b)** An illustration of Lemma 2: An evader at position  $e$  or  $e'$  can generate the measurement  $b(t)$  because the angle  $\widehat{e p^* e'}$  is less than  $2\alpha$ .

111 *Proof.* The function  $\beta(x)$  is the angle between the two points  $p_1$  and  $p_2$  from the point  $x$ , as shown. First,  
 112 notice if  $x$  is anywhere *left* of the line,  $\ell_1$ , we can move the point toward the centroid of  $p_1$  and  $p_2$  and strictly  
 113 increase the angle  $\beta(x)$ . Thus, the point maximizing  $\beta(x)$  is on the line  $\ell_1$ .

Without loss of generality, let  $p_1$  be at the point  $(d, \frac{s}{2})$  and  $p_2$  be at  $(d, -\frac{s}{2})$ , and let the coordinates of the point  $x$  be  $(0, y)$ . The function  $\beta(x)$  can be expressed as follows.

$$\beta(x) = \tan^{-1} \left( \frac{\frac{s}{2} - y}{d} \right) + \tan^{-1} \left( \frac{\frac{s}{2} + y}{d} \right) \quad (3)$$

114 It can be verified the maximum of the function occurs when  $y = 0$ , corresponding to the point  $x$  being along  
 115 the perpendicular bisector of  $p_1$  and  $p_2$ .  $\square$

116 We are now ready to prove the evader can take either trajectory,  $E$  or  $E'$ , and still generate the same  
 117 measurement sequence  $B$ .

118 **Lemma 2.** Let  $E'$  be the sequence of evader positions given by  $\{(d + t \cos \rho, -t \sin \rho) : t = [1, N]\}$ , and  $E$   
 119 be the sequence of evader positions given by  $\{(d + t \cos \rho, t \sin \rho) : t = [1, N]\}$ . The bearing measurement  
 120 sequence  $B$  described in Algorithm 1 can be generated by an evader following either  $E$  or  $E'$ .

121 *Proof.* As shown in Figure 4, the pursuer at every time step is inside the circle denoted  $C_p(t)$  of radius  $t$   
 122 centered on  $p(0)$ . Let  $\beta(t)$  be the  $\widehat{e(t)p(t)e'(t)}$ . By Lemma 1, the position  $p(t)$  which maximizes the angle  $\beta(t)$   
 123 is at the intersection of the  $x$  axis and the boundary of  $C_p(t)$ . We call this point  $p^*(t)$  and the corresponding  
 124 angle  $\beta^*(t)$ .

Let the distance between  $p^*(t)$  and the line  $\overline{e(t)e'(t)}$  be  $d(t)$ . For all  $t \in [1, N]$  the following holds.

$$d(t) = d(0) + t(\cos \rho - 1) \quad (4)$$

Note the minimum value is at  $t = N$  and  $d(N) > 0$  by design. The separation between  $e(t)$  and  $e'(t)$  is,

$$s(t) = |e(t) - e'(t)| = 2t \sin \rho \quad (5)$$

which is maximized when  $t = N$ . The angle,  $\beta^*(t)$  satisfies the following.

$$\beta^*(t) = 2 \cdot \tan^{-1} \left( \frac{s(t)}{2d(t)} \right) \quad (6)$$

Recall  $\tan^{-1}(x)$  is monotonic in  $x$  and the argument  $\frac{s(t)}{2d(t)}$  is maximized at  $t = N$ . Therefore  $\beta^*(t)$  is maximized when  $t = N$ . By inspecting Figure 2 we see,

$$\beta^*(t) = 2 \cdot \tan^{-1} \left( \frac{d(N) \sin \alpha}{d(N) \cos \alpha} \right) \quad (7)$$

125 which implies  $\beta^*(N) = 2\alpha$ , or  $\beta(t) \leq 2\alpha$  for all  $t \in [1, N]$ .

126 Consider the measurements  $B$  from the evader's simulation (Algorithm 1). Recall each  $b(t)$  was given by  
 127 the angle to the point  $e(t)$  from  $p(t)$ , minus  $\alpha$ . We have just proven the angle  $e(t)\widehat{p(t)}e'(t)$  is less than  $2\alpha$   
 128 for any  $p(t)$ , as illustrated in Figure 4.

129 Thus, the angle between  $b(t)$  and  $e'(t)$  is less than  $\alpha$  for all  $p(t)$  and an evader at  $e'(t)$  can use an offset  
 130 less than  $\alpha$  to generate the same measurement  $b(t)$  for all  $t \in [1, N]$ .  $\square$

131 The previous lemmas shows the evader can always end up in Case 1, either by directly following trajectory  
 132  $E$ , or by following an alternate trajectory  $E'$ , with the choice resolved by the simulation before the first move  
 133 is made by either player. Thus, the ending configuration is as shown in Figure 2. We are now ready to prove  
 134 the first main result of the paper: That each application of the evader's strategy yields a constant-factor  
 135 increase in the distance between the pursuer and evader.

**Lemma 3.** *For any deterministic pursuer strategy,  $\pi_p$ , an evader distance  $d(0)$  away with maximum bearing offset,  $\alpha$ , using Algorithm 1 produces a final separation after  $N$  turns satisfying,*

$$d(N) = \beta \cdot d(0) \quad (8)$$

136 with  $\beta > 1$  when  $\alpha > 0$ .

*Proof.* The proof follows directly from the configuration of the players at the end of the round. As shown in Figure 2,

$$[T_\alpha d(0)]^2 = [d(N) \sin \alpha]^2 + [(T_\alpha - 1)d(0) + d(N) \cos \alpha]^2 \quad (9)$$

After some manipulation, we solve for  $d(N)$  as a function of  $d(0)$  as follows.

$$d(N) = d(0) \left[ \sqrt{\cos^2 \alpha (T_\alpha - 1)^2 + 2T_\alpha - 1} - \cos \alpha (T_\alpha - 1) \right] \quad (10)$$

137 We call the term in brackets in the previous equation  $\beta$ , and note  $T_\alpha > 1$  by design making  $\beta > 1$  for any  
 138 positive  $\alpha$ .  $\square$

139 We now consider *repeated* applications of the evader's strategy e.g., after playing for some large time,  $t$ .  
 140 Since each round increases the separation between the players by a constant factor, and the length of the  
 141 round is also proportional to the separation at the start of the round, we expect a logarithmic number or  
 142 rounds played before any time  $t$ . We combine the logarithmic number of rounds played before a given time  
 143  $t$ , with the exponential increase to prove the following: the distance will increase at a rate proportional to  
 144 the time  $t$ .

**Theorem 1.** *For any deterministic pursuer strategy,  $\pi_p$ , an evader using repeated applications of the strategy given in Algorithm 1 increases the distance to the pursuer,  $d(t)$ , at a linear rate. At the end of after  $t$  turns playing, the distance satisfies the following at the end of each evader round.*

$$d(t) \geq \gamma \cdot t + d(0) \quad (11)$$

$$\text{with } \gamma = \left( \sqrt{\frac{2}{1 + \cos \alpha}} - 1 \right) \quad (12)$$



---

**Algorithm 1** Evader Strategy:  $\pi_e(\alpha, d, \pi_p)$ 


---

```

 $T_\alpha \leftarrow \left(1 - \sqrt{\frac{1}{2 + 2 \cos \alpha}}\right)^{-1}$ 
 $\rho \leftarrow \pi - \sin^{-1}((1 - T_\alpha^{-1}) \sin \alpha)$ 
 $\hat{p}(1) \leftarrow (0, 0)$ 
 $B \leftarrow \emptyset$ 
 $N \leftarrow T_\alpha \cdot d$ 
for all  $t \in [1, N)$  do
     $b^* \leftarrow$  orientation of the line connecting  $\hat{p}(t)$  and the point  $(d + t \cos \rho, t \sin \rho)$ 
     $B(t) \leftarrow b^* - \alpha$ 
     $\hat{p}(t + 1) \leftarrow \pi_p(\hat{P}, B)$ 
end for
if  $\hat{p}(N)$  on or below  $\bar{p}e$  then
    for all  $t \in [1, N]$  do
         $e(t) \leftarrow (d + t \cos \rho, t \sin \rho)$ 
        Give measurement  $B(t)$ 
    end for
else
    for all  $t \in [1, N]$  do
         $e(t) \leftarrow (d + t \cos \rho, -t \sin \rho)$ 
        Give measurement  $B(t)$ 
    end for
end if

```

145 *Proof.* Given the result of Lemma 3, we see the first round takes time  $T_\alpha d(0)$ , and produces  $d(1) = \beta d(0)$ .  
 146 Continuing, the  $i^{\text{th}}$  round takes time  $T_\alpha \cdot d(i - 1)$ , and produces end-of-round separation  $d(i) = \beta d(i - 1)$ .  
 147 Or, after expansion back to the first round,  $d(i) = \beta^i d(0)$ .

For any time  $t$ , which falls at the end of  $n$  rounds, the following holds.

$$t = \sum_{i=0}^n T_\alpha \cdot (\beta^i d(0)) \quad (13)$$

Which implies  $n = \log_\beta \left(1 + t \frac{\beta - 1}{T_\alpha \cdot d(0)}\right)$ . At the end of these  $n$  rounds, the separation is,

$$d(t) = d(0) \beta^n \quad (14)$$

$$= d(0) \beta^{\log_\beta \left(1 + t \frac{\beta - 1}{T_\alpha \cdot d(0)}\right)} \quad (15)$$

$$= d(0) + t \frac{\beta - 1}{T_\alpha} \quad (16)$$

148 Note the constant  $\beta$  contains both  $T_\alpha$  and  $\alpha$ . It can be verified the choice of  $T_\alpha$  given in Equation (1)  
 149 maximizes  $\frac{\beta - 1}{T_\alpha}$  when  $\alpha \in (0, \frac{\pi}{2}]$ , and produces a rate of increase as given in the theorem statement.  $\square$

### 3 The Lion and Man Game

151 We now investigate the effect of uncertain bearing measurements in the context of the classical Lion-and-  
 152 Man game. The game is played in a circular arena. At the beginning of the game, the pursuer specifies a  
 153 starting location  $p(0)$  followed by the evader choosing a starting location  $e(0)$ . The game proceeds in turns.

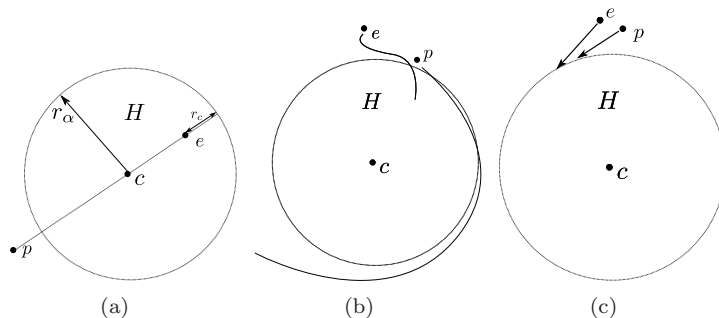


Figure 5: **a)** The lion-and-man starting configuration. At the start of the game, the evader chooses his location diametrically opposite the pursuer’s location. **b)** The three-phase strategy starts when the pursuer enters (or starts within) the *home region*  $H$ , a circle of radius  $r_\alpha$ , or moves to within distance  $2r_c$  of the evader. The boundary of the arena is assumed to be much larger than  $r_\alpha$ , but is upper-bounded in Theorem 2. **c)** After sufficiently increasing the distance between players (Phase 1), and inducing an angular offset (Phase 2) the evader dashes back to the home region, re-entering without being captured (Phase 3).

154 First, the pursuer obtains a measurement, i.e. the angle to the evader,  $b(t)$ . As before, due to uncertainty,  
 155  $b(t) = b^*(t) + \alpha(t)$  where  $b^*$  is the orientation of the line through the two players, adjusted by  $\alpha(t)$ , an  
 156 angle of the evader’s choosing up to absolute value  $\alpha$ . The pursuer moves to a point contained inside the  
 157 arena and within the step size which is normalized to one unit. We again assume the pursuer must choose a  
 158 deterministic strategy  $\pi_p$  which is a function of the bearing measurements and his prior locations. After the  
 159 pursuer’s move, if the evader is within a fixed radius ( $r_c$ ) the pursuer wins the game. Otherwise, the evader  
 160 may make his move of up to one unit distance in the same way as the pursuer.

161 To win the Lion-and-Man game, the evader (the man) must maintain a separation from the pursuer (the  
 162 lion) which is greater than the capture radius ( $r_c$ ), regardless of the pursuer strategy. We will show it is  
 163 possible: For any given  $\alpha > 0$ , there exist environments in which the evader can forever escape a deterministic  
 164 pursuer.

165 The evader’s strategy proceeds in three phases, each illustrated in Figure 5. During the first phase, the  
 166 evader will move away from the lion and repeatedly use Algorithm 1 to increase the separation between the  
 167 players. In the second phase, the evader will execute a local maneuver, which ensures the man is offset from  
 168 the line between the center of the arena and the pursuer by an angle greater than  $\frac{\alpha}{3}$ . In Phase 3, the evader  
 169 will exploit the separation between itself and the lion to make a dash toward the center of the arena. When  
 170 it is “close enough” to the center, the evader will start over from Phase 1. In the remainder of the paper we  
 171 will show the evader can repeat these three steps indefinitely while avoiding capture, regardless of the lion’s  
 172 strategy.

### 173 3.1 Evader’s Winning Strategy

174 We now present the strategy for the evader to win the Lion-and-Man game. We present the technical details  
 175 of the three phases as separate proofs (Corollary 1 and Lemmas 4- 5). Following, we show the three phases,  
 176 taken together, produce a repeatable evader strategy in Theorem 2.

177 The starting configuration is depicted in Figure 5(a). As shown, let  $c$  be the center of the arena. The  
 178 evader will identify a *home region*  $H$  inside the arena where  $H$  is a circle centered at  $c$ . The radius of  $H$ ,  
 179  $r_\alpha$  is a function of  $\alpha$  and  $r_c$  and specified in Theorem 2. Let the pursuer start at location  $p$ , at distance  $r_p$   
 180 from  $c$ . The evader will choose to start inside the boundary of  $H$  at distance  $r_\alpha - 2r_c$  diametrically opposite  
 181 the pursuer. Before the first Phase, the evader will simply wait until the pursuer enters  $H$ . The evader will  
 182 move directly away from the pursuer’s current location until he reaches the boundary of  $H$ . At this time,  
 183 Phase 1 begins.

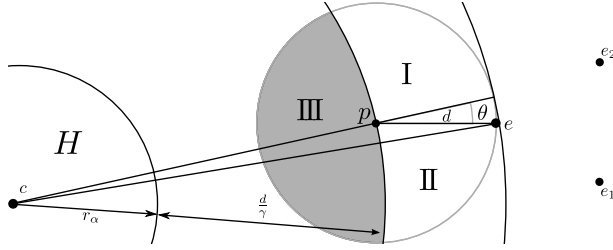


Figure 6: At the end of Phase 1 the pursuer  $p$  and evader  $e$  are separated by a distance  $d$  given in Corollary 1. At the start of Phase 2, the evader examines the angle  $\theta$ . If  $\theta > \frac{\alpha}{3}$  the evader can move on to Phase 3. Otherwise, he chooses his next move based on the next pursuer location, in region I, II, or III, as stated in Lemma 4

184 The beginning of Phase 1 is illustrated in Figure 5(a). In Phase 1, the evader will repeatedly apply the  
 185 distance-increasing strategy from Section 2 (Algorithm 1). Each application of the strategy is called a round,  
 186 and Phase 1 ends when enough rounds have been completed to increase the separation between the players  
 187 to a desired distance  $d > \frac{1}{\sin \frac{\alpha}{3}}$ . The key to the analysis of Phase 1 is to show the players do not travel an  
 188 unbounded distance from the center of the arena. Since Theorem 1 provides a lower bound on the separation  
 189 between the players as a function of the number of turns spent, we can bound the number of turns required  
 190 in Phase 1 as follows.

191 **Corollary 1** (Effect of Phase 1). *Let the distance between the pursuer and evader at the start of Phase 1*  
 192 *be  $d(0) \geq r_c$ . After  $T$  turns, the separation is greater than  $d(T) \geq \gamma T$ , where  $\gamma = \frac{1}{\cos \frac{\alpha}{2}} - 1$ , is given in*  
 193 *Theorem 1. For any given desired separation  $d$ ,  $T \leq \frac{d}{\gamma} = d \left( \frac{\cos \frac{\alpha}{2}}{1 - \cos \frac{\alpha}{2}} \right)$  turns are required.*

194 After Phase 1, the players are in the configuration shown in Figure 6. Let the pursuer's maximum  
 195 distance from  $c$  at the end of Phase 1 be  $r_p$ , and let  $C_r$  be the circle of radius  $r_p$  centered on  $c$ . Similarly,  
 196 let  $r_e$  be the maximum distance of the evader from  $c$ . Because the players traveled at most distance  $\frac{d}{\gamma}$  from  
 197 the region  $H$ , we know Phase 1 ensures  $r_p \leq r_\alpha + \frac{d}{\gamma}$ . Since the distance between the players is  $d$ , we know  
 198 Phase 1 also ensures  $r_e \leq r_\alpha + d(1 + \frac{1}{\gamma})$ . The evader will check the angle  $\theta$ , which is the orientation of the  
 199 line  $\overline{pe}$  with respect to the line  $\overline{ce}$  (i.e., the angle  $\pi - \widehat{pce}$ ), as labelled in Figure 6. If  $\theta > \frac{\alpha}{3}$ , the evader will  
 200 move on to Phase 3. Otherwise, the evader must make a local move to create the desired value of  $\theta$ . The  
 201 local move is Phase 2 as described next.

202 First, the evader will wait until the pursuer makes a move outside the circle  $C_p$  or  $\theta \geq \frac{\alpha}{3}$ . While the  
 203 pursuer remains inside  $C_p$ , the evader does not need to take any action, and does not adjust the pursuer's  
 204 bearing measurements from their true value. When the pursuer exits the circle  $C_p$ , and  $\theta$  is still less than  
 205  $\frac{\alpha}{3}$ , the evader will begin a simulate step, exactly as in described in Section 2, for  $d$  turns (just enough time  
 206 for the pursuer to reach the evader's initial location,  $e$ ).

207 Let  $e_1$  and  $e_2$  be two points, offset by  $\pm\alpha$  from the line  $\overline{pe}$  at distance  $d$  from  $e$ . As before, the evader  
 208 constructs the bearing measurement sequence to be the orientation between the current simulated pursuer  
 209 location  $\hat{p}(i)$  and the point distance  $i$  along the line segment  $\overline{ee_2}$ , starting at the point  $e$  when  $i = 0$ . As  
 210 before the bearings are offset by negative  $\alpha$ .

211 Let  $\hat{p}$  be the final pursuer location after the simulated move. First, if  $\hat{p}$  is inside the circle  $C_p$  (in region  
 212 III in Figure 6), the evader does not need to take any action, and will continue to wait in Phase 2. Otherwise,  
 213 we partition the possible locations of  $\hat{p}$  into two sets, I and II, divided by the line  $\overline{ce}$ , as shown in Figure 7(a)  
 214 and 7(b), respectively. If  $\hat{p} \in I$ , the evader will choose to move to  $e_1$ , otherwise he moves to  $e_2$ . In such a  
 215 case, Phase 2 ends when the evader reaches  $e_1$  or  $e_2$  after  $d$  turns. We use the following lemma to show the  
 216 configuration of the players after Phase 2.

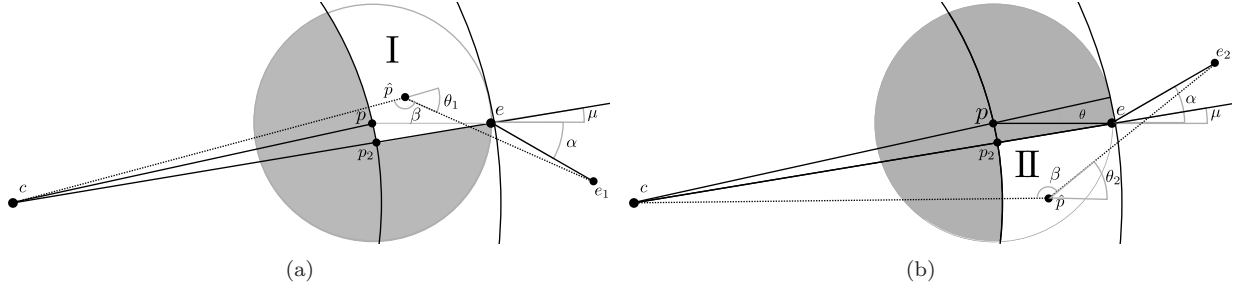


Figure 7: **a and b)** By Lemma 4, the evader can choose to move to location  $e_1$  or  $e_2$ , based on the pursuer's chosen location in region I or II, producing  $\theta_1$  or  $\theta_2$  greater than  $\frac{\alpha}{3}$ , respectively. If the pursuer moves to region III, the evader will remain at position  $e$ .

217 **Lemma 4** (Effect of Phase 2). *Let  $p$  and  $e$  be the pursuer and evader position after Phase 1 as shown in*  
 218 *Figure 7. Consider the point  $\hat{p}$ , at most distance  $d$  from  $p$ , and falling into region I or II (outside the radius*  
 219  *$r_p$ ). For any such  $\hat{p}$  there exists a corresponding point  $\hat{e}$ , at most distance  $d$  from  $e$  such that all of the*  
 220 *following hold.*

- 221 1. *Max  $r_p$ : The distance between  $\hat{p}$  and  $c$  is at most  $d(1 + \frac{1}{\gamma}) + r_\alpha$*
- 222 2. *Max  $r_e$ : The distance between  $\hat{e}$  and  $c$  is at most  $r_p + d = d(2 + \frac{1}{\gamma}) + r_\alpha$*
- 223 3. *Separation: The distance between  $\hat{p}$  and  $\hat{e}$  is at least  $d$ .*
- 224 4. *Angular Offset: The angle  $\theta$ , which is measured between the line  $\overline{\hat{p}\hat{e}}$  and the line  $\overline{c\hat{p}}$  is at least  $\frac{\alpha}{3}$ .*

225 *Proof.* As illustrated in Figure 7, Let  $c$  be the center of the playing environment. Let the pursuer be at  
 226 position  $p$  and radius  $r_p$  from  $c$ , and the evader be at radius  $r_e \geq r_p + d$ . From Corollary 1, we know the  
 227 players travelled at most distance  $\frac{d}{\gamma}$  after exiting  $H$  and the evader is distance  $d$  away.

228 For any pursuer location,  $\hat{p}$ , and evader location  $\hat{e}$ , we notice the first two conditions stated in the theorem  
 229 hold, since the evader and pursuer move at most distance  $d$ . Also note for any  $\hat{p}$  above (resp. below) the  
 230 line  $\overline{ce}$ , the point  $e_1$  (resp.  $e_2$ ) is at least distance  $d$  away, since  $l(\overline{ee_1}) = d$  and  $l(\overline{ee_2}) = d$ . It remains to  
 231 show the evader has achieved an angular offset as stated.

232 Consider case I:  $\hat{p} \in \text{I}$ , and the evader has moved to  $e_1$ , as illustrated in Figure 7(a). Let  $\beta$  be the angle  
 233  $\widehat{e_1\hat{p}c}$ , implying  $\theta_1 = \pi - \beta$ . Of all  $\hat{p} \in \text{I}$ ,  $\beta$  is maximized ( $\theta_1$  minimized) when  $\hat{p} = p_2$ . To see this, draw the  
 234 line  $\overline{ce_1}$ , find its midpoint, and recall from Lemma 1  $\beta$  increases by moving  $\hat{p}$  toward the midpoint. We now  
 235 show  $\theta_1 \geq \frac{\alpha}{3}$ .

236 First find the perpendicular projection of  $e_1$  onto the line  $\overline{ce}$ . The distance of the projection from the point  
 237  $p_2$  is  $d + d \cos(\alpha + \mu)$ . The length of the projection is  $d \sin(\alpha + \mu)$ . Since  $\tan \theta_1 = \frac{d \sin(\alpha + \mu)}{d + d \cos(\alpha + \mu)} = \tan(\frac{\alpha + \mu}{2})$ ,  
 238  $\theta_1 > \frac{\alpha}{2}$ .

239 Consider case II:  $\hat{p} \in \text{II}$ , and the evader has moved to  $e_2$ , as illustrated in Figure 7(b). By a similar  
 240 argument as before, we see  $\beta$  is maximized when  $\hat{p} = p_2$ . We again find the projection of  $e_2$  onto the line  $\overline{ce}$ ,  
 241 which has length  $d \cos(\alpha - \mu)$ , and intersects  $\overline{ce}$  at distance  $d + d \sin(\alpha - \mu)$  from  $p_2$ . Now, we note  $\mu < \theta < \frac{\alpha}{3}$   
 242 by assumption. Therefore  $\tan \theta_2 > \frac{d \sin(\frac{2\alpha}{3})}{d + d \cos(\frac{2\alpha}{3})}$  which implies  $\theta_2 > \frac{\alpha}{3}$ . Thus, all four conditions are proved.  
 243 □

244 To recap the result of Phase 1 and 2, we know the pursuer is inside a circle  $C_p$ , with radius  $r_p \leq$   
 245  $r_\alpha + d(1 + \frac{1}{\gamma})$ , and the evader is inside the circle  $C_e$  with radius  $r_e \leq r_p + d$ . We also know the evader is  
 246 offset from the line  $\overline{cp}$  by an angle at least  $\frac{\alpha}{3}$  and is distance at least  $d$  from the pursuer. The evader will  
 247 now move on to the last phase. Now the evader will move at an angle from the line  $\overline{pe}$ , given by  $\frac{\pi}{2} + \phi$ , where

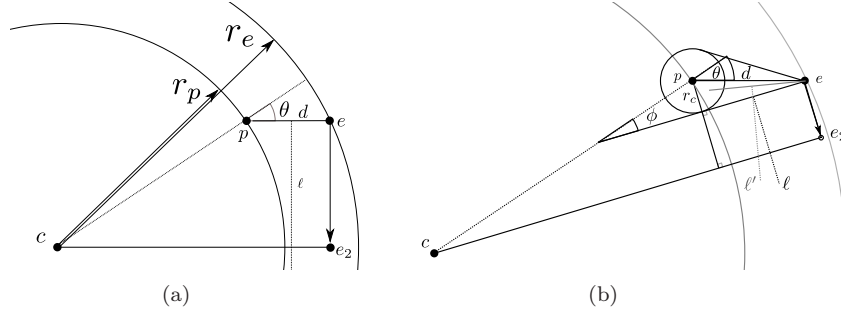


Figure 8: During Phase 2, the evader will move at an angle  $\phi + \frac{\pi}{2}$ , where  $\phi$  is measured with respect to the line from the center of the circle to the point  $p$ . After Phase 2, the evader is at position  $e_2$ . Lemma 4 shows  $\theta \geq \frac{\alpha}{3}$  and bounds  $r_p$  and Lemma 5 bounds the distance from the center to  $e'$ . Note  $\phi = \theta - \sin^{-1} \frac{r_c}{d}$  and  $d$  is chosen such to ensure  $\phi > 0$ .

248  $\phi = \theta - \sin^{-1} \frac{r_c}{d}$ . The angle  $\phi$  is chosen so for any  $r_c$ , there exists a separation  $d$  which makes it possible for  
 249 the evader to move closer to the center of the arena without being captured. This move is called Phase 3,  
 250 and is illustrated in Figure 8.

**Lemma 5** (Effect of Phase 3). *Let  $c$  be the center of the playing circle, and a pursuer with capture radius  $r_c$  be distance  $r_p$  from the  $c$ . Let the evader be distance  $d$  away from the pursuer, and offset from the line between the pursuer and center of the circle by an angle  $\theta$ . The evader can reach a point distance  $r^*$  from the center of the circle without being captured where  $r^*$  satisfies*

$$r^* \leq r_p \cos(\phi) + \sqrt{d^2 - r_c^2} \quad (17)$$

$$\text{with } \phi = \theta - \sin^{-1} \left( \frac{r_c}{d} \right) > 0 \quad (18)$$

251 *Proof.* For simplicity, let us consider the case of  $r_c = 0$  as illustrated in Figure 8(a). The locus of all points  
 252 equidistant from  $p$  and  $e$  is given by the perpendicular bisector of the line  $\overline{pe}$ , which we label  $\ell$ . By travelling  
 253 parallel to  $\ell$  the evader can reach the point  $e_2$  before the pursuer can. Since the line  $\overline{pe}$  and  $\overline{ce_2}$  are parallel,  
 254 we see the angle  $\widehat{pce_2}$  is exactly  $\theta$ . The distance  $l(\overline{pe_2})$  is given by  $r_p \cos \theta + l(\overline{pe}) = r_p \cos \theta + d$ , as desired.

255 In the case of  $r_c > 0$ , the evader modifies his strategy as follows. We observe escaping capture by a  
 256 pursuer with  $r_c > 0$  is the same as escaping any pursuer  $p'$  with  $r_c = 0$ , when the initial position of  $p'$  is at  
 257 most distance  $r_c$  from the point  $p$ . We will find an escape path for the evader along which no  $p'$  which can  
 258 achieve capture.

259 To proceed we draw a line tangent to the circle of radius  $r_c$  and passing through  $e$ . Let the tangent point  
 260 on the circle be  $p_t$ . The evader will travel parallel to the perpendicular bisector of the line segment  $\overline{ep_t}$ ,  
 261 labelled  $\ell$  until he reaches the location closest to  $c$ , labelled  $e_2$  in Figure 8(b).

262 To see the evader can reach  $e_2$  without being captured, consider any pursuer with no capture radius  
 263 ( $r_c = 0$ ) at location  $p'$ , at most distance  $r_c$  from the point  $p$ . Let  $\ell'$  be the perpendicular bisector of the line  
 264  $\overline{ep'}$ . For any  $p' \neq p_t$ , the line  $\ell'$  rotates away from  $e_2$ , leaving  $e_2$  safely on the evader's side. For any  $p'$  closer  
 265 to  $e$ , the line  $\ell'$  moves closer to  $e_2$ , but for  $e_2$  to lie on  $\ell'$ ,  $p'$  must be coincident with  $e$ . Since the evader  
 266 enters Phase 2 with separation  $d > 0$ , this is not possible.

267 To find the inner radius, note  $\overline{ce_2}$  is parallel with the line passing through  $e$  and tangent to the capture  
 268 circle, implying  $\widehat{pce_2}$  is exactly  $\theta - \sin^{-1} \left( \frac{r_c}{d} \right)$ . The distance  $l(\overline{pe_2})$  is given as stated in the lemma.

269 □

270 All that remains is to show the evader is now back in the home region,  $H$ .

271 **Theorem 2.** Let  $\phi$  be  $\frac{\alpha}{3} - \sin^{-1} \frac{r_c}{d}$ , and let  $d$  be any constant greater than  $\frac{r_c}{\sin \frac{\alpha}{3}}$ . Let  $\gamma$  be the constant  
272  $\left(\sqrt{\frac{2}{1+\cos \alpha}} - 1\right)$  from Theorem 1. An evader beginning inside a circle  $H$  of radius  $r_\alpha = \frac{d(1+\frac{1}{\gamma}) \cos \phi + \sqrt{d^2 - r_c^2}}{1 - \cos \phi}$   
273 can, after all three phases described, return to the circle  $H$  without being captured.

*Proof.* By assumption, the radius of  $H$  is  $r_\alpha = \frac{d(1+\frac{1}{\gamma}) \cos \phi + \sqrt{d^2 - r_c^2}}{1 - \cos \phi}$ . After Phase 2, as stated in Lemma 4, the pursuer is at most distance  $r_p = r_\alpha + d(1 + \frac{1}{\gamma})$  from the center,  $c$ .

$$r_p = \frac{d(1 + \frac{1}{\gamma}) \cos \phi + \sqrt{d^2 - r_c^2}}{1 - \cos \phi} + d(1 + \frac{1}{\gamma}) \quad (19)$$

We now apply Lemma 5 to find the inner radius reachable by the evader. Let the inner radius be  $r^*$ .

$$r^* = \left[ \frac{d(1 + \frac{1}{\gamma}) \cos \phi + \sqrt{d^2 - r_c^2}}{1 - \cos \phi} + d(1 + \frac{1}{\gamma}) \right] \cos \phi + \sqrt{d^2 - r_c^2} \quad (20)$$

After distributing  $\cos \phi$ , and the denominator, we have,

$$r^* = \frac{d(1 + \frac{1}{\gamma}) \cos^2 \phi + \sqrt{d^2 - r_c^2} \cos \phi + d(1 + \frac{1}{\gamma}) \cos \phi(1 - \cos \phi) + \sqrt{d^2 - r_c^2}(1 - \cos \phi)}{1 - \cos \phi} \quad (21)$$

$$r^* = \frac{d(1 + \frac{1}{\gamma}) \cos \phi(\cos \phi + 1 - \cos \phi) + \sqrt{d^2 - r_c^2}(\cos \phi + 1 - \cos \phi)}{1 - \cos \phi} \quad (22)$$

$$r^* = \frac{d(1 + \frac{1}{\gamma}) \cos \phi + \sqrt{d^2 - r_c^2}}{1 - \cos \phi} \quad (23)$$

274 Thus, at the end of Phase 3, assuming  $r_\alpha$ ,  $\phi$ , and  $d$  are chosen as stated, the evader is again inside the home  
275 region,  $H$  and is outside the capture radius of the pursuer.  $\square$

276 After entering the home region,  $H$ , the evader can continue to move directly away from the pursuer's  
277 location. Upon exiting  $H$ , the game has reset, and the evader can start over in Phase 1, repeating indefinitely.

## 278 4 Concluding Remarks

279 In this paper, we studied pursuit-evasion games in which the pursuer can obtain only uncertain bearing  
280 measurements. We showed that the evader can exploit this uncertainty and change the outcome of the game  
281 in his favor in two classical games. These are the first theoretical results on pursuit-evasion with bearing  
282 uncertainty.

283 In the games we considered, there is only one pursuer and the players have the same maximum speed. It  
284 is likely that the evader can be captured by either increasing the number of pursuers or the maximum speed  
285 of the (single) pursuer. Obtaining bounds for these versions are interesting avenues for future research.

286 Another possibility is to allow randomization in pursuer strategies. The evader strategy in the open  
287 plane can be modified to work against randomized strategies since this game is infinite. In the lion-and-  
288 man game however, there is a finite winning strategy when the pursuer can measure the true location. By  
289 discretizing the circle, we can obtain a finite set containing all pursuit strategies. No matter which strategy  
290 the evader plays, at least one element of this set would capture the evader and this strategy can be "guessed"  
291 using randomization. Hence the evader can be captured even without any measurements. The capture time  
292 resulting from this argument would be exponential in the duration of the game. In [6], it was shown that  
293 the capture time is indeed exponential when the game takes place on arbitrary graphs. Whether this bound  
294 can be improved when bearing measurements are available is another avenue for future research.

## References

- [1] J. E. Littlewood, *Littlewood's miscellany*. Cambridge University Press, 1986.
- [2] T. H. Chung, G. A. Hollinger, and V. Isler, "Search and pursuit-evasion in mobile robotics: A survey," *Autonomous robots*, vol. 31, no. 4, pp. 299–316, 2011.
- [3] P. Tokekar, E. Branson, J. Vander Hook, and V. Isler, "Tracking aquatic invaders," *IEEE Robotics and Automation Magazine*, vol. 20, no. 3, pp. 447–452, September 2013.
- [4] L. Alonso, A. S. Goldstein, and E. M. Reingold, "Lion and man: upper and lower bounds," *ORSA Journal on Computing*, vol. 4, no. 4, pp. 447–452, 1992.
- [5] G. Röte, "Pursuit-evasion with imprecise target location," in *Proceedings of the fourteenth annual ACM-SIAM Symposium on Discrete algorithms (SODA)*. Society for Industrial and Applied Mathematics, 2003, pp. 747–753.
- [6] V. Isler and N. Karnad, "The role of information in the cop-robber game," *Theoretical Computer Science*, vol. 399, no. 3, pp. 179–190, 2008.

## A Notation

- $p$  The pursuer's current position.  $p(t)$  is used for time-indexed positions.
- $e$  The evaders's current position.  $e(t)$  is used for time-indexed positions.
- $b^*(t)$  the orientation of the line  $\ell$  in a fixed coordinate frame at the start of turn  $t$ .
- $\widehat{abc}$  the angle formed by the points  $a$ ,  $b$ , and  $c$
- $\overline{ab}$  the line passing through points  $a$  and  $b$
- $l(\overline{ab})$  the length of the line segment connecting points  $a$  and  $b$
- $b(t)$  The pursuer's measurement of the orientation of  $\overline{pe}$ , as adjusted by the evader during turn  $t$ .
- $\alpha$  The evader's maximum angular disturbance of  $b(t)$
- $C(a, r)$  a circle centered on point  $a$  of radius  $r$

## B Constant Definitions

- $r_c$  The capture radius of the pursuer, as used in the Lion-and-Man game.
- $T_\alpha$  The optimal duration of Algorithm 1 is given by  $T_\alpha \cdot d$ , where  $d$  is the distance between the players at the start of the algorithm. Defined in Equation 1
- $\gamma$   $\left(\sqrt{\frac{2}{1+\cos\alpha}} - 1\right)$  The rate at which an evader can increase the distance between himself and a pursuer, defined in Equation 12.
- $\alpha$  The maximum angular disturbance in the pursuer's bearing measurement.
- $\rho$  The evader's escape angle during the Open Plane Pursuit game. Defined in Equation 2 to be  $\pi - \sin^{-1}((1 - T_\alpha^{-1}) \sin \alpha)$
- $\theta$  The angle between  $\overline{cp}$  and  $\overline{pe}$ , or  $\widehat{cpe}$ .
- $\phi$  The evader's escape angle during Phase 3 of the Lion and Man game. Defined in Theorem 2